separate, sequential reactions, each of which probably opens a binding site to permit one Na^+ to escape. Each charge component has well defined characteristics. The slowest appears to reflect strongly electrogenic (equivalent valence, $z \approx 1$; Fig. 2b) release of the first Na^+, through ~70% of the membrane field, in a reaction that is rate limited by the slow (~100 to 1,400 s^{-1}) major E_1-P ↔ P-E_2 conformational change, which itself seems relatively electroneutral; this slow component shows low sensitivity to $[Na]_o$ (Fig. 2b) but has strongly temperature-sensitive rates[5], revealing an enthalpic activation energy of ~80 kJ mol^{-1} (10–20 °C; not shown; see ref. 13). Like the slow component, the medium-speed (~6,000 to 20,000 s^{-1}) component also has a steeply voltage-dependent charge magnitude ($z \approx 1$; Fig. 4d), and a relaxation rate that increases with $[Na]_o$ at negative potentials and shows a high activation energy (~70 kJ mol^{-1}; not shown) and, hence, probably reflects the reaction that de-occludes the second Na^+. The fast component mirrors the time course of the distributed membrane capacitance transient and so must reflect charge transitions with rates $\geq 10^6$ s^{-1}, appropriate for rapid Na^+ release through an access channel, but still possibly rate limited by a minor conformational change that de-occludes the final Na^+; consistent with their high speed, these relaxations show little temperature sensitivity (not shown). In further contrast to the slow and medium-speed components, the fast charge movement has extremely weak voltage sensitivity (note simple scaling of the fast component amplitude with potential over a 160-mV range in Fig. 4c), and it is seen in virtual isolation at very low $[Na]_o$ (≤25 mM; not shown), indicating that it may reflect release of the final Na^+ ion(s) from a relatively high-affinity site(s) on P-E_2 (see refs 8, 9, 12). Our failure to observe any comparably high-speed charge movement displaying the strong voltage sensitivity of the medium-speed and slow components, despite exploring a broad range of $[Na]_o$ and voltage, argues (see ref. 8) that there must be negligible steady-state occupancy of the narrow (high-field) access-channel conformation P-$E_2(Na_2)$·Na, which we propose (Fig. 4a) is ultimately responsible for those slower charge relaxations; this in turn implies that both rate constants leading away from that state (k_{-1} and k_2 in Fig. 4a) are relatively large.

The strictly sequential nature of the three charge components shown here indicates that the three Na^+ may be released from the Na^+/K^+ pump in a fixed order. Ordered occlusion/de-occlusion of two K^+ by kidney microsomal Na^+/K^+-ATPase[14] and sequential occlusion, translocation and release of the two Ca^{2+} ions transported by the sarcoplasmic reticulum Ca^{2+}-ATPase[15] have been detected using isotopes and rapid filtration techniques (time resolution ~10 ms), but the far higher time resolution and sensitivity of the electrical recording methods used here permit extraction of finer molecular kinetic detail[8,12,16]. Closer examination, using these methods, of the interactions of extracellular Na^+ ions with their binding sites within the Na^+/K^+ pump will now be required to discern the precise molecular rearrangements that surround these principal charge movements in the Na^+/K^+ transport cycle. □

Methods

Giant axons from the squid *Loligo pealei* were voltage clamped[17], internally dialysed and externally superfused at 20–22 °C with Cl^--free solutions[7,10] designed to restrict the pump to Na^+ de-occlusion/release steps (Fig. 1). Intracellular (in mM; pH adjusted with HEPES): 80 Na-HEPES, 57 *N*-methyl-D-glucamine(NMG)-HEPES, 50 glycine, 50 phenylpropyltriethylammonium-sulphate, 5 dithiothreitol, 2.5 1,2-bis(2-aminophenoxy)ethane-N,N,N′,N′-tetraacetic acid (BAPTA), 15 Mg-HEPES, 5 Tris-ATP, 5 phospho(enol)pyruvate tri-Na^+-salt and 5 phospho-L-arginine mono-Na^+-salt. Extracellular (in mM): 400 Na-isethionate, 75 Ca-sulphamate, 1 3,4-diaminopyridine, 2×10^{-4} tetrodotoxin, 5 Tris-HEPES and 0.05 EDTA (pH 7.7). Osmolality of all solutions was ~930 mOsmol kg^{-1}. To lower $[Na]_o$, Na-isethionate was replaced by tetramethylammonium-sulphamate or NMG-sulphamate. Voltage pulses were generated and currents recorded using a 16-bit PC44 A-D/D-A converter board (Innovative Technologies) with software developed in-house. Currents were filtered at 12.5–200 kHz, then sampled at 20 kHz–2 MHz. Current records were sometimes acquired after subtraction of appropriately amplified small current signals, obtained in a voltage range where pump-mediated charge movement tended towards saturation, to minimize currents from linear membrane capacitance. Pump current was determined as current sensitive to 100 μM H_2DTG[10].

Received 22 September; accepted 17 December 1999.

1. Post, R. L., Hegyvary, C. & Kume, S. Activation by adenosine triphosphate in the phosphorylation kinetics of sodium and potassium ion transport adenosine triphosphatase. *J. Biol. Chem.* **247,** 6350–6540 (1972).
2. Beaugé, L. A. & Glynn, I. M. Occlusion of K ions in the unphosphorylated sodium pump. *Nature* **280,** 510–512 (1979).
3. Garraham, P. J. & Glynn, I. M. The behaviour of the sodium pump in red cells in the absence of external potassium *J. Physiol.* **192,** 161–174 (1967).
4. Fendler, K., Grell, E., Haubs, M. & Bamberg, E. Pump currents generated by the purified Na^+K^+-ATPase from kidney on black lipid membranes. *EMBO J.* **4,** 3079–3085 (1985).
5. Nakao, M. & Gadsby, D. C. Voltage dependence of Na translocation by the Na/K pump. *Nature* **323,** 628–630 (1986).
6. Läuger, P. *Electrogenic Ion Pumps* (Sinauer, Sunderland, MA, 1991).
7. Gadsby, D. C., Rakowski, R. F. & De Weer, P. Extracellular access to the Na,K pump: pathway similar to ion channel. *Science* **260,** 100–103 (1993).
8. Hilgemann, D. W. Channel-like function of the Na,K pump probed at microsecond resolution in giant membrane patches. *Science* **263,** 1429–1432 (1994).
9. Heyse, S., Wuddel, I., Apell, H. J. & Sturmer, W. Partial reactions of the Na,K-ATPase: determination of rate constants. *J. Gen. Physiol.* **104,** 197–240 (1994).
10. Rakowski, R. F., Gadsby, D. C. & De Weer, P. Stoichiometry and voltage-dependence of the sodium pump in voltage-clamped, internally-dialyzed squid giant axon. *J. Gen. Physiol.* **93,** 903–941 (1989).
11. Läuger, P. & Apell, H. J. Transient behaviour of the Na^+/K^+-pump: microscopic analysis of nonstationary ion-translocation. *Biochim. Biophys. Acta* **944,** 451–464 (1988).
12. Wuddel, I. & Apell, H. J. Electrogenicity of the sodium transport pathway in the Na,K-ATPase probed by charge-pulse experiments. *Biophys. J.* **69,** 909–921 (1995).
13. Friedrich, T. & Nagel, G. Comparison of Na^+/K^+-ATPase pump currents activated by ATP concentration or voltage jumps. *Biophys. J.* **73,** 186–194 (1997).
14. Forbush, B. Rapid release of 42K or 86Rb from two distinct transport sites on the Na,K-pump in the presence of Pi or vanadate. *J. Biol. Chem.* **262,** 11116–11127 (1987).
15. Inesi, G. Characterization of partial reactions in the catalytic and transport cycle of sarcoplasmic reticulum ATPase. *J. Biol. Chem.* **262,** 16338–16342 (1987).
16. Lu, C.-C. *et al.* Memtrane transport mechanisms probed by capacitance measurements with megahertz voltage clamp. *Proc. Natl Acad. Sci. USA* **92,** 11220–11224 (1995).
17. Bezanilla, F., White, M. M. & Taylor, R. E. Gating currents associated with potassium channel activation. *Nature* **296,** 657–659 (1982).

Acknowledgements

This work was supported by grants from the NIH. M.H. was supported in part by the Grass Foundation, and J.W. held a HHMI Postdoctoral Research Fellowship for Physicians.

Correspondence and requests for materials should be addressed to D.C.G. (e-mail: gadsby@rockvax.rockefeller.edu), or to M.H. (e-mail: miguel_holmgren@hms.harvard.edu).

The 21-nucleotide *let-7* RNA regulates developmental timing in *Caenorhabditis elegans*

Brenda J. Reinhart*†, Frank J. Slack*†‡, Michael Basson‡§, Amy E. Pasquinelli*, Jill C. Bettinger‡#, Ann E. Rougvie#, H. Robert Horvitz§ & Gary Ruvkun*

** Department of Molecular Biology, Massachusetts General Hospital, and Department of Genetics, Harvard Medical School, Boston, Massachusetts 02114, USA*

§ Howard Hughes Medical Institute, Department of Biology, Massachusetts Institute of Technology, Cambridge, Massachusetts 02139, USA

 # Department of Genetics, Cell Biology and Development, University of Minnesota, St Paul, Minnesota 55108, USA

† These authors contributed equally to this work

The *C. elegans* heterochronic gene pathway consists of a cascade of regulatory genes that are temporally controlled to specify the timing of developmental events[1]. Mutations in heterochronic genes cause temporal transformations in cell fates in which stage-specific events are omitted or reiterated[2]. Here we show that *let-7* is a heterochronic switch gene. Loss of *let-7* gene activity causes reiteration of larval cell fates during the adult stage, whereas increased *let-7* gene dosage causes precocious expression of adult fates during larval stages. *let-7* encodes a temporally regulated 21-nucleotide RNA that is complementary to elements in the 3′ untranslated regions of the heterochronic genes *lin-14*, *lin-28*, *lin-41*, *lin-42* and *daf-12*, indicating that expression of these genes may be directly controlled by *let-7*. A reporter gene bearing the *lin-41* 3′ untranslated region is temporally regulated in a *let-7*-dependent manner. A second regulatory RNA, *lin-4*, negatively regulates *lin-14* and *lin-28* through RNA–RNA interactions with their 3′ untranslated regions[3,4]. We propose that the sequential stage-specific expression of the *lin-4* and *let-7* regulatory RNAs triggers transitions in the complement of heterochronic regulatory proteins to coordinate developmental timing.

‡ Present addresses: Axys Pharmaceuticals, South San Francisco, California 94080, USA (M.B.); Ernest Gallo Clinic and Research Center, UCSF, Emeryville, California 94608, USA (J.C.B.); Department of MCDB, Yale University, New Haven CT 06520, USA (F.J.S.).

To identify new heterochronic genes, we carried out a genetic screen for mutations that suppress the synthetic sterile phenotype of a strain bearing the *lin-14(n179)* and *egl-35(n694)* mutations. We separated candidate suppressor mutations from the *lin-14* and *egl-35* mutations and examined each mutant for heterochronic defects. Out of 36 suppressor mutations isolated from animals carrying 44,000 mutagenized haploid genomes, the mutation *n2853* caused the strongest retarded heterochronic defects in a *lin14*(+) background (Fig. 1c; Table 1) and a temperature-sensitive adult lethal phenotype associated with vulval bursting. Another suppressor mutation, *mg279*, failed to complement *n2853* and caused a weak retarded phenotype (Table 1). We genetically mapped *n2853* and *mg279* and found that of the lethal mutations in the same region, *let-7(mn112)* (ref. 5) displayed heterochronic (Table 1) and lethal phenotypes (93% lethal, $n = 60$) nearly identical to that of *n2853*. *let-7(mn112)* is not temperature sensitive and failed to complement both *n2853* and *mg279*.

The first evidence of a *let-7* heterochronic defect is at the L4-to-adult moult. Hypodermal blast cells normally divide at each larval stage and at the adult stage exit the cell cycle, fuse with neighbouring hypodermal seam cells and generate cuticular alae[6] (Fig. 1a). In *let-7(n2853)* animals, the blast cell lineages were normal through the L3-to-L4 moult, but at the L4-to-adult moult, they reiterated larval patterns of cell division and failed to generate alae (Fig. 1a; Table 1). *let-7(n2853)* mutant animals reared at the permissive temperature underwent a supernumerary moult to a fifth larval stage, L5 (56%, $n = 26$). At the L5-to-adult moult, seam cells exited the cell cycle, fused with neighbouring seam cells, and produced alae (100%, $n = 10$ animals). The opposite phenotype resulted from over-expressing *let-7*. Increasing *let-7* gene dosage on a transgenic array caused hypodermal cells to precociously exit the cell cycle and terminally differentiate after the L3-to-L4 moult (83%, $n = 18$ animals). The opposite heterochronic phenotypes caused by reducing or increasing *let-7* activity indicate that *let-7* may function as a temporal switch between larval and adult fates.

let-7 acts upstream of the heterochronic gene *lin-29*, a zinc-finger transcription factor that specifies adult-specific patterns of cell lineage and cell differentiation[2,7]. In wild-type animals, LIN-29 protein is expressed during the L4 and adult stages in hypodermal cells[8]. Consistent with the delay of adult differentiation by one stage in *let-7(n2853)* animals, LIN-29 expression in the hypodermis of L4 stage *let-7* animals was reduced relative to wild type, but expressed at normal levels at the L5 stage (Fig. 1b–d). Thus, *let-7* is necessary for the upregulation of LIN-29 expression in the hypodermis during the L4 stage, which in turn specifies adult cell fates.

The retarded alae phenotype caused by *let-7* mutations was partially suppressed by precocious mutations in the genes *lin-41*, *lin-42*, *lin-14* and *lin-28* (Table 1). For these epistasis experiments, we used the strong *let-7* allele *mn112*, which by molecular criteria completely eliminates gene function (see below). Mutations in *lin-41* and *lin-42* cause precocious expression of adult fates during late larval stages but do not affect L1 and L2 stage fates[9,10]. Thus, like *let-7* mutations, *lin-41* and *lin-42* mutations specifically affect late larval stage development and these three genes may function at about the same time during development. The *let-7* retarded heterochronic (Table 1) and lethal (F. J. Slack *et al.*, manuscript in preparation) phenotypes were partially suppressed by *lin-41* and *lin-42* mutations; conversely, the precocious alae phenotypes of *lin-41* and *lin-42* mutants were partially suppressed by a *let-7* mutation (Table 1). Although other interpretations are possible, these data are consistent with a model in which *lin-41* and *lin-42* are negatively regulated by *let-7*. Molecular analysis (see below) suggests that regulation by *let-7* may be direct.

Unlike *let-7* mutations, *lin-14* and *lin-28* mutations affect early larval development[2], suggesting that *let-7* functions later than *lin-14* and *lin-28*. For example, *lin-28*-null mutants delete L2 fates, but double mutant combinations with *let-7* did not suppress this early defect (Table 1). However, the reiteration of larval fates caused by the *let-7*-null mutation was partially suppressed by the precocious expression of adult fates caused by *lin-28* or *lin-14* null mutations

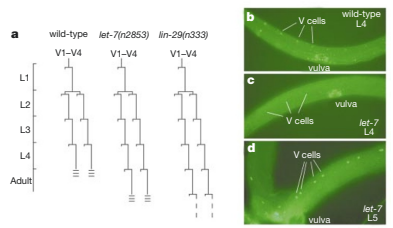

Figure 1 The *let-7* heterochronic phenotype. **a**, Lineage of the lateral hypodermal cells V1, V2, V3 and V4 in wild-type[8], *let-7(n2853)* and *lin-29(n333)* animals[2]. L3 and L4 stage V cell lineages are equivalent in hermaphrodites and cannot be distinguished. **b**, Wild-type L4 stage animal with LIN-29 expression in the lateral hypodermis and vulva. **c**, *let-7(n2853)* L4 stage animal with LIN-29 expression reduced in V cells but at normal levels in vulval cells. **d**, An L5 stage *let-7(n2853)* animal showing accumulation of LIN-29 at high levels one stage later than wild-type animals.

Table 1 Phenotype of *let-7* mutants and interactions with other heterochronic mutants

Strain	Percentage of animals with adult lateral alae*			
	L3 moult		L4 moult	
Wild-type (N2)	0	(25)	100	(25)
let-7(mn112) unc-3(e151)	0	(20)	0	(20)
let-7(n2853) 15 °C	0	(20)	0	(20)
let-7(n2853) 25 °C	0	(30)	0	(20)
let-7(mg279)	0	(20)	100†	(24)
lin-41(ma104)	54†	(48)	100	(45)
lin-41(ma104); let-7(mn112) unc-3(e151)	0	(18)	70	(20)
lin-42(n1089)	90†	(72)	100	(58)
lin-42(n1089); let-7(mn112) unc-3(e151)	13	(66)	31	(86)
lin-14(n536 n540)	100	(25)	100	(25)
lin-14(n536 n540) let-7(mn112) unc-3(e151)	44†	(36)	70	(46)
lin-14(n179) 25 °C	100	(38)	100	(28)
lin-14(n179) let-7(mn112) unc-3(e151) 25 °C	18	(32)	30	(129)
lin-28(n719)	100	(20)	100	(20)
lin-28(n719); let-7(mn112); unc-3(e151)‡	7†	(60)	17†	(58)
lin-4(e912)	0	(20)	0	(20)
lin-4(e912); let-7(mn112) unc-3(e151)	0	(20)	0	(40)

All strains were grown at 20° unless otherwise indicated.
* The number of animals is given in parentheses.
† Some animals had patches of alae rather than continuous alae, indicating a mix of larval fates for some V cells and adult fates for others. Percentage of animals with patches: 29% of *let-7(mg279)* adults; 25% of *lin-41(ma104)* L4s; 28% of *lin-42(n1089)* L4s; 33% of *lin-14(n536n540) let-7(mn112) unc-3(e151)* L4s; 7% of *lin-28(n719); let-7(mn112) unc-3(e151)* L4s; and 17% of lin-28 (n719); *let-7(mn112) unc-3(e151)* adults.
‡ In *lin-28; let-7* animals, the postdeirid cells derived from the V5 blast cell during the L2 stage were absent in L4-stage animals ($n = 5$), suggesting that the deletion of V cell L2 fates caused by the *lin-28(n719)* null mutation was not suppressed.